Tunable Spin-Crossover Behavior in Polymethylated Bis(indenyl)chromium(II) Complexes: The Significance of Benzo-Ring Substitution

M. Brett Meredith,[†] Jeffrey A. Crisp,[†] Erik D. Brady,[†] Timothy P. Hanusa,*[,†] Gordon T. Yee,*[,‡] Maren Pink,[§] William W. Brennessel,[§] and Victor G. Young, Jr.[§]

Department of Chemistry, Vanderbilt University, Nashville, Tennessee 37235, Department of Chemistry, Virginia Polytechnic Institute and State University, Blacksburg, Virginia 24061, and X-ray Crystallographic Laboratory, Chemistry Department, University of Minnesota, Minneapolis, Minnesota 55455

Received May 24, 2008

The magnetic properties of monomeric bis(indenyl)chromium(II) complexes are sensitive to the relative orientation of the ligands (staggered, eclipsed, or gauche), regardless of whether such a conformation is imposed by sterically bulky substituents or is a consequence of crystal-packing forces. The staggered monomethylated compound (2-$MeC_9H_6)_2Cr$ has previously been found to display a high-spin state in the solid state and solution, whereas the monomeric (1-$MeC_9H_6)_2Cr$ is eclipsed in the solid state and exhibits spin-crossover behavior over a wide temperature range. The present work examines the synthesis, structures, and magnetic properties of polymethylated indenyl complexes containing two, three, and five substituents on the indenyl ligand. Methyl groups on the benzo portion appear to be critical in supporting a low-spin ground state; the order of the preference to exist as a low-spin complex is approximately (2,4,5,6,7-$Me_5C_9H_2)_2Cr$ > (2,4,7-$Me_3C_9H_4)_2Cr$ ≈ (4,7-$Me_2C_9H_5)_2Cr$ > (1,2,3-$Me_3C_9H_4)_2Cr$ > (1-$MeC_9H_6)_2Cr$ ≥ (2-$MeC_9H_6)_2Cr$. The (2,4,7-$Me_3C_9H_4)_2Cr$ complex crystallizes with two conformations in the unit cell: one with an eclipsed geometry and the other staggered. When the temperature is raised from 173 to 293 K, the staggered form undergoes approximately 3 times the bond length increase as the eclipsed form. The difference is attributed to the symmetry-driven preference of the staggered configuration for the high-spin state.

Introduction

There is considerable interest in the synthesis of transition metal compounds whose magnetic properties can be influenced by external agents.[1] In the case of spin-crossover complexes, transitions between high- and low-spin states can be induced by temperature, pressure, and light,[2] and the specific metal and ligand requirements for supporting such transitions have received intensive investigation. Effective control of spin-state transitions could ultimately lead to applications in switching devices, magnetic storage, and photonic systems.[3]

Among the ligand-based forces that can drive spin-state changes are steric interactions,[4] hydrogen bonding,[5] and $\pi-\pi$ bonding interactions.[6] Only recently have the symmetry effects found in substituted bis(indenyl)chromium(II) complexes been added to this list. Such effects rely on the interdependence of orbital occupancy and ligand conformation in bis(indenyl)metal complexes.[7] An orbital analysis of Ind′$_2$Cr complexes indicates that in a staggered, centrosymmetric complex (e.g., the red-purple (1,3-(*i*-Pr)$_2C_9H_5)_2Cr$[8] or (1-(*t*-Bu)$C_9H_6)_2Cr$;[9] see Figure 1 for the numbering convention), a high-spin ($S = 2$) state is preferred, as the ungerade combinations of the indenyl π orbitals cannot interact with the d orbitals of chromium, leaving d

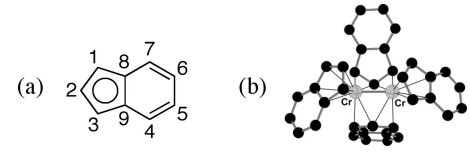

Figure 1. (a) Numbering scheme for the indenyl anion. (b) Solid-state structure of {Ind$_2$Cr}$_2$.[10]

* To whom correspondence should be addressed. E-mail: t.hanusa@vanderbilt.edu (T.P.H.).
[†] Vanderbilt University.
[‡] Virginia Polytechnic Institute and State University.
[§] University of Minnesota.

(1) Sato, O.; Tao, J.; Zhang, Y.-Z. *Angew. Chem., Int. Ed.* **2007**, *46*, 2152–2187.
(2) (a) Gütlich, P.; Hauser, A.; Spiering, H. *Angew. Chem.* **1994**, *106*, 2109–2141. (b) Gütlich, P.; Garcia, Y.; Woike, T. *Coord. Chem. Rev.* **2001**, *219−221*, 839–879. (c) Real, J. A.; Gaspar, A. B.; Munoz, M. C. *Dalton Trans.* **2005**, 2062–2079.
(3) (a) Kahn, O. *Molecular Magnetism*; VCH: New York, 1993. (b) *Topics in Current Chemistry: Spin Crossover in Transition Metal Compounds I-III*; Gütlich, P., Goodwin, H. A., Eds.; Springer: Berlin, 2004; Vol. 233−235.
(4) Hays, M. L.; Burkey, D. J.; Overby, J. S.; Hanusa, T. P.; Yee, G. T.; Sellers, S. P.; Young, V. G., Jr *Organometallics* **1998**, *17*, 5521–5527.
(5) Gütlich, P. *Struct. Bonding* **1981**, *44*, 83–195.
(6) (a) Gallois, B.; Real, J. A.; Hauw, C.; Zarembowitch, J. *Inorg. Chem.* **1990**, *29*, 1152–1158. (b) Real, J. A.; Gallois, B.; Granier, T.; Suez-Panama, F.; Zarembowitch, J. *Inorg. Chem.* **1992**, *31*, 4972–4979. (c) Zhong, Z. J.; Tao, J.-Q.; Yu, Z.; Dun, C.-Y.; Liu, Y.-J.; You, X.-Z. *J. Chem. Soc., Dalton Trans.* **1998**, 327–328.
(7) Calhorda, M. J.; Veiros, L. F *Coord. Chem. Rev.* **1999**, *185−186*, 37–51.
(8) Overby, J. S.; Hanusa, T. P.; Sellers, S. P.; Yee, G. T. *Organometallics* **1999**, *18*, 3561–3562.
(9) Brady, E. D.; Overby, J. S.; Meredith, M. B.; Mussman, A. B.; Cohn, M. A.; Hanusa, T. P.; Yee, G. T.; Pink, M. *J. Am. Chem. Soc.* **2002**, *124*, 9556–9566.

10.1021/om800473z CCC: $40.75
Publication on Web 09/27/2008

electrons in singly occupied, metal-centered orbitals.[9] This analysis has been supported by the isolation of Ind'_2Cr species with more sterically demanding substituents (e.g., *t*-Bu, $SiMe_3$) at the 1- and 3-positions of the indenyl ligand. In such compounds, the ligands have been forced into ~90° (gauche) orientations, leaving green, low-spin ($S = 1$) compounds. The reduction of symmetry allows mixing of the indenyl π orbitals with the metal d orbitals, which increases the HOMO−LUMO gap and produces low-spin configurations.[9]

That the conformation−spin-state relationship in bis(indenyl) complexes was not recognized earlier stems from the fact that the first bis(indenyl)chromium complex to be structurally characterized was the green heptamethylindenyl derivative ($(Ind^{7Me})_2Cr$).[11] The average Cr−C bond length (2.18(2) Å) was consistent with that in known bis(cyclopentadienyl)chromium complexes (~2.1−2.2 Å), and magnetic measurements indicated that the metal was low-spin from 5 to 235 K, as are almost all chromocenes and chromium(II) organometallic complexes with π-bound ligands.[12,13] In retrospect, the low-spin state of $(Ind^{7Me})_2Cr$ can be seen to reflect strong electron donation from the peralkylated ring, which despite symmetry restrictions sufficiently increases the HOMO−LUMO gap to change the spin state.

In principle, any substituent that breaks the centrosymmetry of a bis(indenyl)Cr(II) complex could lead to non-high-spin complexes. We have begun a survey of complexes containing methyl-substituted indenyl ligands[14] and have found that a single methyl group at the 1- or 2-position of the indenyl ligand is enough to disrupt the dimerization observed in the unsubstituted parent complex (Figure 1b).[10] Red bis(2-methylindenyl)chromium(II), $(Ind^{Me-2})_2Cr$, displays a staggered geometry in the solid state and is a high-spin complex both in solution and as a solid down to 25 K. In solution, the 1-methyl analogue $(Ind^{Me-1})_2Cr$ is high-spin from 183 to 298 K, but in the solid state, the complex adopts an eclipsed geometry and displays spin-crossover behavior, with a magnetic moment rising from 2.87 μ_B at 20 K (consistent with $S = 1$) to 4.1 μ_B by 275 K, representing an incomplete spin transition to the $S = 2$ state.

Much less is known about how substitution on the benzo portion of the indenyl ligand affects the properties of associated bis(indenyl)chromium(II) complexes. Other than the fully methylated complex,[11] the only attempt to prepare a complex with substitution on the benzo portion led to the isolation of the dinuclear $(Ind^{Me-4})_3Cr_2Cl$ complex.[14] We report here a study of polymethylated Ind'_2Cr complexes that further illuminates the interrelationship among ligand conformation, electron donation, and substitution patterns on the magnetic properties of the compounds. Such knowledge is valuable in the pursuit of tunable magnetism in systems such as charge-transfer salts[15] and in predicting and controlling metal center reactivity.

Experimental Section

General Considerations. Unless mentioned otherwise, all manipulations were performed with the rigorous exclusion of air and moisture using Schlenk or glovebox techniques. ^{1}H NMR spectra were obtained on a Bruker DPX-300 spectrometer at 300 MHz. Elemental analyses were performed by Desert Analytics (Tucson, AZ). Melting points were determined in sealed capillaries. Mass spectra were obtained using a Hewlett-Packard 5890 Series II gas chromatograph/mass spectrometer.

Materials. All the methylated indenes were prepared by variations on standard Friedel−Crafts acylation−alkylation reactions. Specifically, 4,7-dimethylindene was prepared from *p*-xylene and 3-chloropropanoyl chloride according to the literature procedure.[16] 2,4,7-Trimethylindene was prepared from *p*-xylene and methacryloyl chloride, using $AlCl_3$ slurried in CS_2 in place of a solution of polyphosphoric acid;[17] 2,4,5,6,7-pentamethylindene[18] was prepared analogously, but starting with 1,2,3,4-tetramethylbenzene instead of *p*-xylene, and 1,2,3-trimethylindene was prepared from tiglic acid and benzene.[19] Anhydrous chromium(II) chloride was purchased from Strem Chemicals and used as received. Potassium hexamethyldisilazide ($K[N(SiMe_3)_2]$) was purchased from Aldrich. The indenes were converted into their potassium salts by treatment with $K[N(SiMe_3)_2]$ in toluene; 2,4,5,6,7-pentamethylindene was also converted into its lithium derivative by reaction with *n*-BuLi in hexanes. THF, toluene, and hexanes were distilled under nitrogen from potassium benzophenone ketyl.[20] Toluene-d_8 was vacuum-distilled from Na/K (22/78) alloy and stored over type 4A molecular sieves prior to use.

Magnetic Measurements. Variable-temperature solution magnetic susceptibility measurements were performed on a Bruker DRX-400 spectrometer using the Evans NMR method.[21] A small sample (5−9 mg) of the paramagnetic material was dissolved in toluene-d_8 in a 1.0 mL volumetric flask. The solution was thoroughly mixed, and approximately 0.5 mL was placed in a NMR tube containing a toluene-d_8 capillary. The calculations required to determine the number of unpaired electrons based on the data collected have been described elsewhere.[22]

Solid-state magnetic susceptibility data were obtained on a Quantum Designs MPMS SQUID magnetometer. The sample was cooled in zero field and measured upon warming from 1.8 to 300 K. To handle the extremely air- and moisture-sensitive compounds, the previously described sample holder was used;[4] the diamagnetic susceptibility of the sample holder was accepted as the average value of the measurements on several identical sample holders. The diamagnetic correction for each complex was estimated from Pascal's constants.

Synthesis of Bis(4,7-dimethylindenyl)chromium(II), $(Ind^{2Me-4,7})_2Cr$. Anhydrous $CrCl_2$ (0.500 g, 4.07 mmol) was added to a 125 mL Erlenmeyer flask along with a magnetic stirring bar and 30 mL of THF. $K[Ind^{2Me-4,7}]$ (1.483 g, 8.15 mmol) was dissolved in 10 mL of THF and the solution added dropwise to the flask with stirring. The mixture initially turned dark green and then black, and it was stirred overnight. The solvent was removed under

(10) Heinemann, O.; Jolly, P. W.; Krüger, C.; Verhovnik, G. P. J. *Organometallics* **1996**, *15*, 5462–5463.
(11) O'Hare, D.; Murphy, V. J.; Kaltsoyannis, N. *J. Chem. Soc., Dalton Trans.* **1993**, 383–392.
(12) (a) König, E.; Schnakig, R.; Kremer, S.; Kanellakopulos, B.; Kleuze, R. *Chem. Phys.* **1978**, *27*, 331–336. (b) Overby, J. S.; Schoell, N. J.; Hanusa, T. P. *J. Organomet. Chem.* **1998**, *560*, 15–19. (c) Sitzmann, H.; Schar, M.; Dormann, E.; Kelemen, M. *Z. Anorg. Allg. Chem.* **1997**, *623*, 1850–1852.
(13) Robbins, J. L.; Edelstein, N.; Spencer, B.; Smart, J. C. *J. Am. Chem. Soc.* **1982**, *104*, 1882–1893.
(14) Meredith, M. B.; Crisp, J. A.; Brady, E. D.; Hanusa, T. P.; Yee, G. T.; Brooks, N. R.; Kucera, B. E.; Young, V. G., Jr. *Organometallics* **2006**, *25*, 4945–4952.
(15) Crisp, J. A.; Meredith, M. B.; Hanusa, T. P.; Wang, G.; Brennessel, W. W.; Yee, G. T. *Inorg. Chem.* **2005**, *44*, 172–174.
(16) Piccolrovazzi, N.; Pino, P.; Consiglio, G.; Sironi, A.; Moret, M. *Organometallics* **1990**, *9*, 3098–3105.
(17) Kaminsky, W.; Rabe, O.; Schauwienold, A. M.; Schupfner, G. U.; Hanss, J.; Kopf, J. *J. Organomet. Chem.* **1995**, *497*, 181–193.
(18) Klemm, H.; Zell, R.; Shabtai, J. S. *J. Org. Chem.* **1974**, *39*, 698–701.
(19) Ready, T. E.; Chien, J. C. W.; Rausch, M. D. *J. Organomet. Chem.* **1999**, *583*, 11–27.
(20) Perrin, D. D.; Armarego, W. L. F. *Purification of Laboratory Chemicals*,3rd ed.; Pergamon: Oxford, U.K., 1988.
(21) (a) Evans, D. F. *J. Chem. Soc.* **1959**, 2003–2005. (b) Grant, D. H. *J. Chem. Educ.* **1995**, *72*, 39–40. (c) Sur, S. K *J. Magn. Reson.* **1989**, *82*, 169–173. (d) Loeliger, J.; Scheffold, R. *J. Chem. Educ.* **1972**, *49*, 646–647.
(22) Hays, M. L. Ph.D. Dissertation, Vanderbilt University, 1996.

vacuum, and 50 mL of hexanes was added to dissolve the chromium complex. The mixture was filtered through a medium-porosity glass frit, and the filtrate was collected in a 250 mL Schlenk flask, which was placed in a −30 °C freezer. After 48 h, dark green crystals of $(Ind^{2Me\text{-}4,7})_2Cr$ were observed and isolated by cannulation of the mother liquor on a Schlenk line. The crystals were dried under vacuum and brought into the glovebox (0.283 g, 21%): mp 155−160 °C. Anal. Calcd for $C_{22}H_{22}Cr$: C, 78.08; H, 6.55. Found: C, 77.84; H, 6.55. Solution magnetic susceptibility (μ_{eff}^{298K}, μ_B): 3.4.

Synthesis of Bis(1,2,3-trimethylindenyl)chromium(II), $(Ind^{3Me\text{-}1,2,3})_2Cr$. $CrCl_2$ (0.376 g, 3.06 mmol) and $K[Ind^{3Me\text{-}1,2,3}]$ (1.20 g, 6.12 mmol) were placed in a 125 mL Erlenmeyer flask equipped with a magnetic stirring bar. Approximately 40 mL of THF was added, immediately producing a dark green solution. The mixture was stirred overnight. By the following day, the solution had become deep purple. The solvent was removed under vacuum to leave a dark purple solid. Approximately 30 mL of hexanes was added, and all insoluble impurities were removed by filtration over a medium-porosity frit. The filtrate was collected in a 250 mL Schlenk flask and placed in a −30 °C freezer. After 16 h, purple crystals of $(Ind^{3Me\text{-}1,2,3})_2Cr$ had formed. The mother liquor was separated from the crystalline solid by cannulation on a Schlenk line. The crystals were dried under vacuum and taken into the glovebox for isolation (0.221 g, 20% yield): mp 234−238 °C. Anal. Calcd for $C_{24}H_{26}Cr$: C, 78.66; H, 7.15; Cr, 14.19. Found: C, 78.37; H, 7.15; Cr, 13.99. Solution magnetic susceptibility ($\mu_{eff}^{T(K)}$, μ_B): 4.3^{188}, 4.4^{248}, 4.4^{298}.

Synthesis of Bis(2,4,7-trimethylindenyl)chromium(II), $(Ind^{3Me\text{-}2,4,7})_2Cr$. $CrCl_2$ (0.376 g, 3.06 mmol) and $K[Ind^{3Me\text{-}2,4,7}]$ (1.20 g, 6.12 mmol) were placed in a 125 mL Erlenmeyer flask equipped with a magnetic stirring bar. Approximately 40 mL of THF was added, immediately producing a brown solution. The mixture was stirred overnight, and the solvent was removed under vacuum to leave a brown solid. Approximately 50 mL of hexanes was added, and all insoluble impurities were removed by filtration over a medium-porosity frit. The filtrate was collected in a 250 mL Schlenk flask and placed in a −30 °C freezer. After 48 h, blocklike brown crystals of $(Ind^{3Me\text{-}2,4,7})_2Cr$ had formed. The mother liquor was separated from the crystalline solid by cannulation on a Schlenk line. The crystals were dried under vacuum and taken into the glovebox to be isolated (0.550 g, 49% yield): mp 105−108 °C. Anal. Calcd for $C_{24}H_{26}Cr$: C, 78.66; H, 7.15; Cr, 14.19. Found: C, 78.41; H, 7.34; Cr, 13.81. Solution magnetic susceptibility ($\mu_{eff}^{T(K)}$, μ_B): 3.3^{198}, 3.4^{208}, 3.5^{218}, 3.5^{228}, 3.6^{238}, 3.7^{248}, 3.7^{258}, $3.8^{268-298}$, $3.9^{318-378}$.

Synthesis of Bis[2,4,5,6,7-pentamethylindenyl]chromium(II), $(2,4,5,6,7\text{-}Me_5C_9H_2)_2Cr$. $CrCl_2$ (0.060 g, 0.49 mmol) and $Li[2,4,5,6,7\text{-}Me_5C_9H_2]$ (0.188 g, 0.976 mmol) were placed in a flask equipped with a magnetic stirring bar. THF (30 mL) was added, immediately producing a dark brown solution. After 3 h, the solvent was removed under vacuum to leave a red-purple solid. Toluene (2 mL) was added, and all insoluble impurities were removed by filtration over a pipet packed with glass wool and Celite 521. The reddish brown filtrate was collected in a small flask that was left loosely capped in order to allow for slow evaporation. After 8 h, small green crystals were observed and the flask was left undisturbed for 48 h. The remaining filtrate was removed by decantation, and the crystals were dried briefly under vacuum to afford deep green $(2,4,5,6,7\text{-}Me_5C_9H_2)_2Cr$ (0.084 g, 41% yield): mp 125 °C. Comparable results were obtained by starting with $K[2,4,5,6,7\text{-}Me_5C_9H_2]$. Anal. Calcd for $C_{28}H_{34}Cr$: C, 79.58; H, 8.11; Cr, 12.30. Found: C, 79.19; H, 7.86; Cr, 11.92. Solution magnetic susceptibility ($\mu_{eff}^{T(K)}$, μ_B): 3.3^{244}, 3.3^{252}, 3.4^{262}, 3.5^{272}, 3.5^{282}, 3.5^{292}.

Computational Details. Geometry optimizations and frequency calculations were performed using the Gaussian 03 suite of programs.[23] Density functional theory was employed with the use of the TPSSh functional, which is based on the meta-generalized gradient approximation (MGGA) of Tao, Perdew, and Staroverov, with the admixture of 10% exact (Hartree−Fock) exchange;[24] it has been demonstrated to give good results with transition-metal systems.[25] Calculations used the standard 6-31+G(d) Pople basis sets (for Cr, this is (23s,18p,5d,1f)/[6s,6p,3d,1f][26]). In the case of the indenyl anions, some comparative calculations were conducted with the B3LYP functional[27] and the aug-cc-pVTZ basis set.

General Procedures for X-ray Crystallography. A suitable crystal of each sample was located, attached to a glass fiber, and mounted on a Siemens Smart system for data collection at various temperatures. Data collection and structure solution for all molecules were conducted at the X-ray Crystallography Laboratory at the University of Minnesota. The intensity data were corrected for absorption (SADABS). All calculations were performed using the current SHELXTL suite of programs.[28] Final cell constants were calculated from a set of strong reflections measured during the actual data collection. Relevant crystal and data collection parameters for each of the compounds are given in Table 1.

The space groups were determined on the basis of systematic absences (where applicable) and intensity statistics. A direct-methods solution was calculated that provided most of the non-hydrogen atoms from the *E* map. Several full-matrix least-squares/difference Fourier cycles were performed that located the remainder of the non-hydrogen atoms. All non-hydrogen atoms were refined with anisotropic displacement parameters. All hydrogen atoms were placed in ideal positions and refined as riding atoms with relative isotropic displacement parameters.

X-ray Crystallography of $(Ind^{2Me\text{-}4,7})_2Cr$. The space group *Cc* was determined on the basis of systematic absences and intensity statistics. The space group was later confirmed with PLATON[29] to be certain that space group *C*2/*c* was not a possibility. The refinement required modeling for inversion twinning (74:26).

X-ray Crystallography of $(Ind^{3Me\text{-}1,2,3})_2Cr$. Crystals of $(Ind^{3Me\text{-}1,2,3})_2Cr$ were obtained from a concentrated hexanes solution that had been cooled to −30 °C. The space group $P\bar{1}$ was determined as described in the General Procedures. The metal lies on an inversion center, so that only half of the molecule is unique. There is both pseudomerohedral and nonmerohedral (rotational) twinning in the same crystalline specimen.

X-ray Crystallography of $(Ind^{3Me\text{-}2,4,7})_2Cr$ (173 and 293 K). Crystals of $(Ind^{3Me\text{-}2,4,7})_2Cr$ were obtained from a concentrated hexanes solution that had been cooled to −30 °C. Data were collected on separate crystals at 173 and 293 K. The space group $P2_1/c$ was determined as described in the General Procedures. There are two conformations observed in the unit cell. One molecule is found as eclipsed, and the other is found as staggered; the chromium lies on an inversion center in the staggered conformer, leaving only half of the molecule unique.

X-ray Crystallography of $(2,4,5,6,7\text{-}Me_5C_9H_2)_2Cr$. Crystals of $(2,4,5,6,7\text{-}Me_5C_9H_2)_2Cr$ were collected by preparing a concentrated

(23) Frisch, M. J., Gaussian 03, Revision C.02.
(24) Staroverov, V. N.; Scuseria, G. E.; Tao, J.; Perdew, J. P. *J. Chem. Phys.* **2003**, *119*, 12129–12137.
(25) Furche, F.; Perdew, J. P. *J. Chem. Phys.* **2006**, *124*, 044103/1–044103/27.
(26) Rassolov, V. A.; Pople, J. A.; Ratner, M. A.; Windus, T. L. *J. Chem. Phys.* **1998**, *109*, 1223–1229.
(27) Becke, A. D. *Phys. Rev. A* **1988**, *38*, 3098–3100. (b) Lee, C.; Yang, W.; Parr, R. G. *Phys. Rev. B* **1988**, *37*, 785–789. (c) Miehlich, B.; Savin, A.; Stoll, H.; Preuss, H. *Chem. Phys. Lett.* **1989**, *157*, 200–206.
(28) SHELXTL, version 6.1; Bruker Analytical X-Ray Systems, Madison, WI, 2000.
(29) Spek, A. L. *Acta Crystallogr.* **1990**, *A46*, C34.
(30) (a) Spek, A. L. PLATON: A Multipurpose Crystallographic Tool; Utrecht University, Utrecht, The Netherlands, 2002. (b) Trnka, T. M.; Bonanno, J. B.; Bridgewater, B. M.; Parkin, G. *Organometallics* **2001**, *20*, 3255–3264.

Table 1. Crystal Data and Summary of X-ray Data Collection

	$(Ind^{2Me\text{-}4,7})_2Cr$ (173 K)	$(Ind^{3Me\text{-}1,2,3})_2Cr$ (173 K)	$(Ind^{3Me\text{-}2,4,7})_2Cr$ (173 K)	$(Ind^{3Me\text{-}2,4,7})_2Cr$ (293 K)	$(2,4,5,6,7\text{-}Me_5C_9H_2)_2Cr$ (173 K)
formula	$C_{22}H_{22}Cr$	$C_{24}H_{26}Cr$	$C_{24}H_{26}Cr$	$C_{24}H_{26}Cr$	$C_{28}H_{34}Cr$
formula wt	338.40	366.45	366.45	366.45	422.55
color of cryst	dark green	purple	brown	brown	green
cryst dimens, mm	0.36 × 0.32 × 0.12	0.45 × 0.28 × 0.15	0.42 × 0.26 × 0.23	0.45 × 0.40 × 0.40	0.25 × 0.18 × 0.08
space group	*Cc*	$P\bar{1}$	$P2_1/c$	$P2_1/c$	*C*2/*c*
cell dimens					
a, Å	15.3746(14)	7.372(4)	15.256(4)	15.492(4)	11.101(2)
b, Å	18.3542(16)	8.565(5)	9.663(3)	9.721(2)	13.664(2)
c, Å	12.656(1)	−8.586(5)	19.712(5)	19.969(4)	14.302(2)
α, deg		69.977(8)			
β, deg	108.440(2)	74.027(8)	96.277(4)	96.296(8)	93.237(2)
γ, deg		73.589(9)			
V, Å^3	3388.0(5)	478.9(5)	2888.7(13)	2989.1(12)	2165.9(4)
Z	8	1	6	6	4
calcd density, Mg/m^3	1.327	1.271	1.264	1.221	1.296
abs coeff, mm^{-1}	0.672	0.600	0.597	0.577	0.540
F(000)	1424	194	1164	1164	904
radiation type (*λ*, Å)	Mo Kα (0.710 73)	Mo Kα (0.710 73)	Mo Kα (0.710 73)	Mo Kα (0.710 73)	Mo Kα (0.710 73)
temp, K	173(2)	173(2)	173(2)	293(2)	173(2)
limits of data collection	1.78 ≤ *θ* 25.05°	2.58 *θ* ≤ 25.20°	2.08 *θ* ≤ 27.56°	2.05 *θ* ≤ 25.02°	2.37 ≤ *θ* 27.50°
index ranges	−18 ≤ *h* ≤ 18, −21 ≤ *k* ≤ 21, −15 ≤ *l* ≤ 11	−8 ≤ *h* ≤ 8, −9 ≤ *k* ≤ 10, 0 ≤ *l* ≤ 10	−19 ≤ *h* ≤ 19, 0 ≤ *k* ≤ 12, 0 ≤ *l* ≤ 25	−18 ≤ *h* ≤ 18, 0 ≤ *k* ≤ 11, 0 ≤ *l* ≤ 23	−14 ≤ *h* ≤ 14, −16 ≤ *k* ≤ 17, −18 ≤ *l* ≤ 17
total no. of rflns collected	10 472	3994	34 000	21 887	9424
no. of unique rflns	5033 (R_{int} = 0.0346)	1699 (R_{int} = 0.0347)	6633 (R_{int} = 0.0382)	5263 (R_{int} = 0.0366)	2488 (R_{int} = 0.0887)
transmission factors	0.7939−0.9237	0.7741−0.9154	0.7877−0.8750	0.7814−0.8022	0.8769−0.9581
no. of data/restraints/params	5033/2/424	1699/0/119	6633/0/349	5263/0/349	2488/0/137
R indices ($I > 2\sigma(I)$)	R = 0.0364, R_w = 0.0835	R = 0.0600, R_w = 0.1575	R = 0.0336, R_w = 0.0901	R = 0.0394, R_w = 0.1033	R = 0.0847, R_w = 0.2238
R indices (all data)	R = 0.0458, R_w = 0.0893	R = 0.0644, R_w = 0.1678	R = 0.0447, R_w = 0.0986	R = 0.0604, R_w = 0.1188	R = 0.1044, R_w = 0.2341
goodness of fit on F^2	1.042	1.019	1.046	1.027	1.129
max/min peak in final diff map, e/Å^3	0.251/−0.194	1.950/−0.439	0.333/−0.247	0.283/−0.274	1.658/−0.599

toluene solution, which was allowed to evaporate slowly at room temperature. Three major sections of frames were collected with 0.30° steps in *ω* and at three different *ϕ* settings with a detector position of −28° in 2*θ*; the frames showed streaks along *c**. The space group *C*2/*c* was determined as specified in the General Procedures, and the chromium atom lies on a special position (twofold). A residual electron density of 1.6 e/Å^3 was observed at a distance of 3.4 Å from the metal. It is possible that a small amount of impurity or a modulation of the structure with no obvious period is present in the crystal.

Results

Synthesis of Substituted Bis(indenyl)chromium(II) Complexes. All the polymethylindenes ($HInd^{2Me\text{-}4,7}$, $HInd^{3Me\text{-}2,4,7}$, $HInd^{3Me\text{-}1,2,3}$, 2,4,5,6,7-$Me_5C_9H_3$) were readily deprotonated by $K[N(SiMe_3)_2]$ in toluene (eq 1) or *n*-BuLi in hexanes (for 2,4,5,6,7-$Me_5C_9H_3$) to form the solid indenides. Two equivalents of the indenide salt was allowed to react with anhydrous chromium(II) chloride in THF (eq 2). The resulting bis(indenyl)chromium(II) complexes were crystallized either by slow evaporation of solvent from a saturated solution or by cooling of a concentrated solution to approximately −30 °C. The complexes are indefinitely stable at room temperature under a nitrogen atmosphere. Although they are soluble enough to obtain estimates of their magnetic susceptibility, completely interpretable proton NMR spectra were not obtained.

$$HInd^{xMe} + K[N(SiMe_3)_2] \xrightarrow[-HN(SiMe_3)_2]{\text{toluene}} K[Ind^{xMe}] \qquad (1)$$

$$2\,M[Ind^{xMe}] + CrCl_2 \xrightarrow{\text{THF}} (Ind^{xMe})_2Cr + 2\,MCl \qquad (2)$$

Magnetic Susceptibility Measurements. Crystalline samples of the bis(indenyl) complexes were examined with SQUID magnetometry, and in toluene solution. Figures 1−4 show 1/*χ* and effective magnetic moment values (μ_{eff}) in the solid state as a function of temperature for three of the compounds. SQUID data for the magnetically simpler (2,4,5,6,7-$Me_5C_9H_2)_2Cr$ are given in the Supporting Information.

$(Ind^{2Me\text{-}4,7})_2Cr$. The magnetic moments as a function of temperature for $(Ind^{2Me\text{-}4,7})_2Cr$ indicate that it is a spin-crossover complex (Figure 2). Below 100 K, a plot of 1/*χ* as a function of temperature follows Curie−Weiss behavior with a Weiss constant of Θ = −4.5 K. There is apparently some zero-field splitting exhibited by the complex below 20 K. It is low spin (*S* = 1) for Cr(II) below about 110 K; the effective magnetic moment (2.9−3.1 μ_B) is consistent with the spin-only value for two unpaired electrons (2.83 μ_B). Above this temperature, the effective magnetic moment begins to rise, and by 210 K the complex has a magnetic moment of over 3.5 μ_B. By 300 K, it reaches a moment of 4.0 μ_B. This is lower than the spin-only value for four unpaired electrons (4.90 μ_B) and also lower than

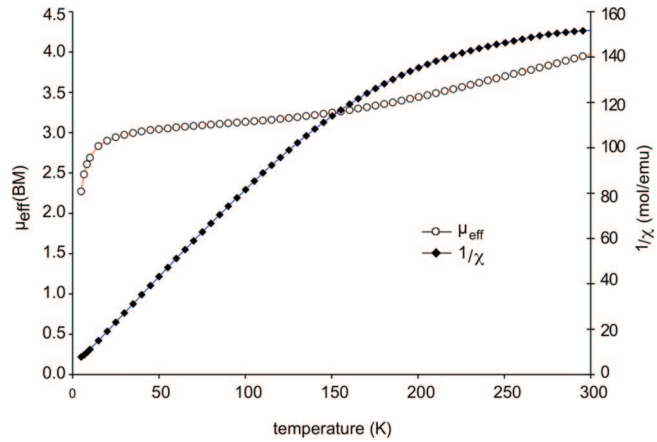

Figure 2. SQUID data for $(Ind^{2Me\text{-}4,7})_2Cr$. Effective magnetic moment (μ_{eff}) and 1/*χ* values (mol/emu) are plotted as a function of temperature.

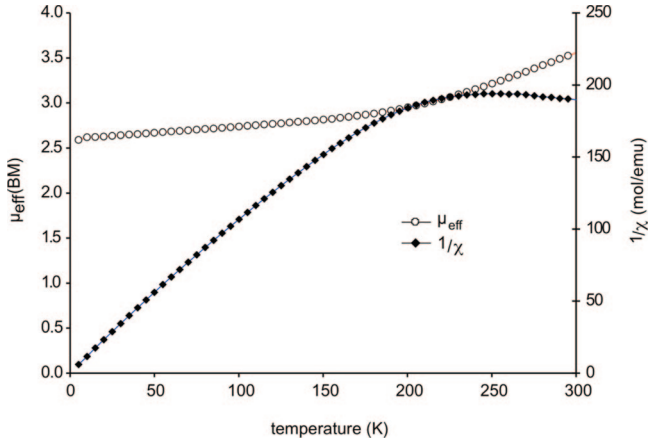

Figure 3. SQUID data for $(Ind^{3Me\text{-}2,4,7})_2Cr$. Effective magnetic moment (μ_{eff}) and $1/\chi$ values (mol/emu) are plotted as a function of temperature.

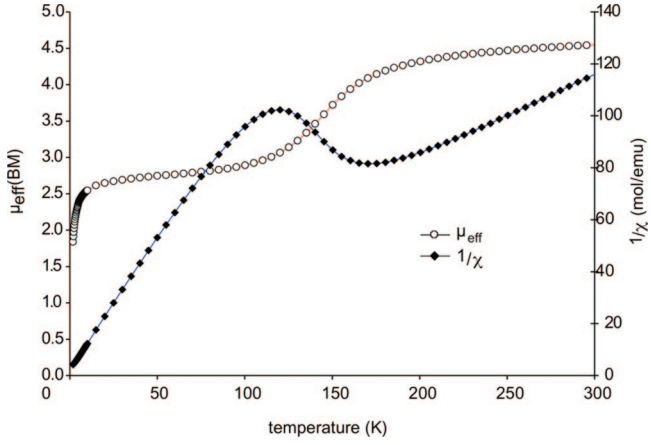

Figure 4. SQUID data for $(Ind^{3Me\text{-}1,2,3})_2Cr$. Effective magnetic moment (μ_{eff}) and $1/\chi$ values (mol/emu) are plotted as a function of temperature.

for other high-spin complexes of this type (ca. 4.4−4.5 μ_B);[8,9] the spin transition should be regarded as incomplete.

Interestingly, in toluene $(Ind^{2Me\text{-}4,7})_2Cr$ displays a magnetic moment of 3.4 μ_B at 298 K, which is lower than the average of the spin-only values for four unpaired electrons (4.9 μ_B) and two unpaired electrons (2.8 μ_B), and is lower than the comparable value observed in the solid state.

$(Ind^{3Me\text{-}2,4,7})_2Cr$. As with $(Ind^{2Me\text{-}4,7})_2Cr$, solid $(Ind^{3Me\text{-}2,4,7})_2Cr$ exhibits spin-crossover behavior, but the spin transition with the latter is even less complete (Figure 3). $(Ind^{3Me\text{-}2,4,7})_2Cr$ is found to be low spin below 200 K and exhibits simple Curie law behavior; the effective moment (2.7−2.9 μ_B) is consistent with the spin-only value for two unpaired electrons. Above 200 K, the complex exhibits spin-crossover behavior but reaches a magnetic moment of only 3.6 μ_B by 300 K. The existence of two conformers in the solid state (see below), one of which is likely to have a stronger preference for a high-spin state than the other, means that the magnetic data are effectively those for a mixture.

Brown solutions of $(Ind^{3Me\text{-}2,4,7})_2Cr$ in toluene exhibit spin-crossover behavior in solution, although shifted to a higher range than in the solid state. The μ_{eff} value is 3.3 μ_B at 188 K (cf. 2.91 μ_B at 190 K in the solid), and the moment rises upon warming in a linear fashion by approximately 0.5 μ_B every 10 K. This trend continues until 288 K, where the moment begins to plateau at 3.8 μ_B and rises only to 3.9 μ_B upon warming to 378 K. The value of 3.8−3.9 μ_B observed between 288 and 378 K is roughly halfway between the spin-only values for two and four unpaired electrons and is noticeably higher than the moment of 3.49 μ_B at 290 K observed in the solid state.

Table 2. Selected Bond Distances (Å) and Angles (deg) for $(Ind^{2Me\text{-}4,7})_2Cr$

Distances			
Cr(1)−C(1)	2.219(3)	Cr(1)−C(12)	2.244(4)
Cr(1)−C(2)	2.150(4)	Cr(1)−C(13)	2.178(4)
Cr(1)−C(3)	2.128(4)	Cr(1)−C(14)	2.121(4)
Cr(1)−C(4)	2.164(4)	Cr(1)−C(15)	2.145(4)
Cr(1)−C(5)	2.251(4)	Cr(1)−C(16)	2.236(4)
Cr(2)−C(23)	2.221(4)	Cr(2)−C(34)	2.209(3)
Cr(2)−C(24)	2.143(4)	Cr(2)−C(35)	2.136(4)
Cr(2)−C(25)	2.118(4)	Cr(2)−C(36)	2.118(4)
Cr(2)−C(26)	2.122(4)	Cr(2)−C(37)	2.150(4)
Cr(2)−C(27)	2.206(4)	Cr(2)−C(38)	2.227(4)
Angles			
inter-C_5 ring plane angle		6.0 (Cr1); 6.7 (Cr2)	
hinge angle[a]		1.5 (Cr1, av); 2.1 (Cr2, av)	
fold angle[a]		2.5 (Cr1, av); 4.4 (Cr2, av)	
twist		8.6 (Cr1); 9.0 (Cr2)	

[a] For definitions of this angle, see ref 11.

$(Ind^{3Me\text{-}1,2,3})_2Cr$. The magnetic moments measured for $(Ind^{3Me\text{-}1,2,3})_2Cr$ indicate that it is a spin-crossover complex (Figure 4). Below 100 K, a plot of $1/\chi$ as a function of temperature follows Curie−Weiss behavior with a Weiss constant of $\Theta = -2.5$ K. There is apparently some zero-field splitting exhibited by the complex below 20 K. The complex is low spin for Cr(II) below 115 K; the effective magnetic moment (2.7−3.0 μ_B) is consistent with the spin-only value for two unpaired electrons. Above 115 K, however, the effective magnetic moment begins to rise, and by 225 K the complex has an effective magnetic moment of over 4.4 μ_B. By 300 K, it reaches a moment of 4.5 μ_B, a value consistent with other high-spin complexes of this type.[8,9]

Dissolution of $(Ind^{3Me\text{-}1,2,3})_2Cr$ in toluene provides a purple solution at room temperature, which is consistent with other substituted high-spin complexes of this type. The spin crossover observed in the solid state has disappeared, as measurements at 188, 248, and 298 K indicate a magnetic moment that varies only between 4.3 and 4.4 μ_B.

$(2,4,5,6,7\text{-}Me_5C_9H_2)_2Cr$. $(2,4,5,6,7\text{-}Me_5C_9H_2)_2Cr$ displays simple Curie law behavior below 175 K. It remains strictly low spin up to 175 K, as evidenced by the effective magnetic moment (2.83−2.86 μ_B) throughout the range from 16 to 175 K. Above 175 K, the effective magnetic moment (and the slope of χT) begins to rise, but the moment reaches just 3.1 μ_B by 275 K; there is only the start of a transition to a higher spin state species. In comparison to $(2,4,5,6,7\text{-}Me_5C_9H_2)_2Cr$, low-spin $(Ind^{7Me})_2Cr$ displayed no evidence of spin equilibrium at any measured temperature (5−235 K).[11] In solution, there is no evidence of spin crossover, as $(2,4,5,6,7\text{-}Me_5C_9H_2)_2Cr$ displays an average μ_B value of 3.5 throughout the temperature range 242−293 K; below 242 K, the compound precipitates from toluene solution. The average value is higher than that found in the solid state but is somewhat lower than that observed for $(Ind^{3Me\text{-}2,4,7})_2Cr$ at the high-temperature end of the scale. It is slightly less than halfway between the spin-only values for two and four unpaired electrons.

Solid-State Structures. All of the complexes possess classic sandwich structures, in either eclipsed or staggered conformations (or both in the case of $(Ind^{3Me\text{-}2,4,7})_2Cr$). Selected bond lengths and angles are given in Tables 2−8; distinctive features of the individual structures are described below.

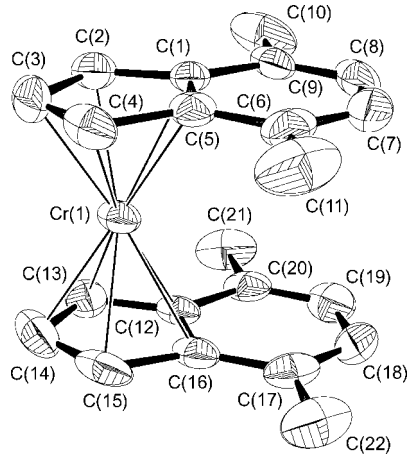

Figure 5. ORTEP drawing of the non-hydrogen atoms of eclipsed $(Ind^{2Me\text{-}4,7})_2Cr$ at 173 K, illustrating the numbering scheme used in the text. Thermal ellipsoids are shown at the 50% level.

$(Ind^{2Me\text{-}4,7})_2Cr$. Crystals of $(Ind^{2Me\text{-}4,7})_2Cr$ were obtained from hexanes as dark green plates. There are two nearly identical molecules in the asymmetric unit; the complex centered on Cr(1) is depicted in Figure 5, which indicates the numbering scheme referred to in the text; selected bond lengths and angles are given in Table 2. No intermolecular π stacking is observed; however, the six-membered rings are nearly eclipsed (twist angles of 8.6 and 9.0° for molecules Cr(1) and Cr(2), respectively) on each molecule. The Cr−C ring distances (average 2.18(1) Å for Cr(1) and 2.17(1) Å for Cr(2)) are consistent with low-spin chromium(II) centers. The two indenyl ligands are bound to the chromium center in an η^5 fashion; the slip parameter[30] (Δ_{M-C} = 0.078 Å for both independent molecules) is typical for low-spin Ind′$_2$Cr complexes (cf. the value for the low-spin $(Ind^{7Me})_2Cr$, Δ_{M-C} = 0.098 Å).[11] The indenyl planes of each molecule are nearly parallel, forming angles of 3.2(1) and 1.9(1)° for Cr(1) and Cr(2), respectively.

$(Ind^{3Me\text{-}1,2,3})_2Cr$. Crystals of $(Ind^{3Me\text{-}1,2,3})_2Cr$ were obtained from cold hexanes as purple needles. Only half of each molecule is unique, as the chromium lies on an inversion center. An ORTEP drawing of the molecule is given in Figure 6, which indicates the numbering scheme referred to in the text; selected bond lengths and angles are given in Table 3.

The Cr−C ring distances observed for this species at 173 K (average 2.239(11) Å) fall between values typically associated with high-spin (av ∼2.30 Å) and low-spin (av <2.21 Å) Ind$_2$Cr complexes.

The ligands are slightly slipped from η^5 coordination; the bridgehead C(8,9)−Cr contacts (average 2.283(7) Å) are longer than the C−Cr distances of C(1) and C(3) (average 2.205(6) Å). This range of Cr−C bonds (Δ_{M-C} = 0.078 Å) is similar to values found in low-spin Ind′$_2$Cr compounds.[11] The methyl substituent at the 2-carbon is displaced from the five-membered ring plane by 3.4°, whereas the methyl substituents at the 1- and 3-carbons are bent out of the plane by less than 0.5°.

$(Ind^{3Me\text{-}2,4,7})_2Cr$. Crystals of $(Ind^{3Me\text{-}2,4,7})_2Cr$ were obtained from cold hexanes as dark brown blocks and examined at 173 and 293 K. Both eclipsed and staggered conformations are found within the unit cell in a 2:1 ratio, respectively. Only half of the staggered conformer is unique, as the chromium lies on an inversion center (Figure 7). The structure of the molecule as determined from data obtained at 173 K is discussed first; ORTEP diagrams of the complex are given as Figures 8 and 9, which indicate the numbering scheme referred to in the text. Drawings for the individual molecules measured at 293 K are available in the Supporting Information. Selected bond lengths and angles for the structures at both temperatures are given in Tables 4−7.

Table 3. Selected Bond Distances (Å) and Angles (deg) for $(Ind^{3Me\text{-}1,2,3})_2Cr$

Distances			
Cr(1)−C(1)	2.209(4)	Cr(1)−C(8)	2.282(5)
Cr(1)−C(2)	2.219(5)	Cr(1)−C(9)	2.283(5)
Cr(1)−C(3)	2.201(5)		

Angles	
inter-C_5 ring plane angle	0.0
hinge angle[a]	5.3
fold angle[a]	4.0

[a] For definitions of this angle, see ref 11.

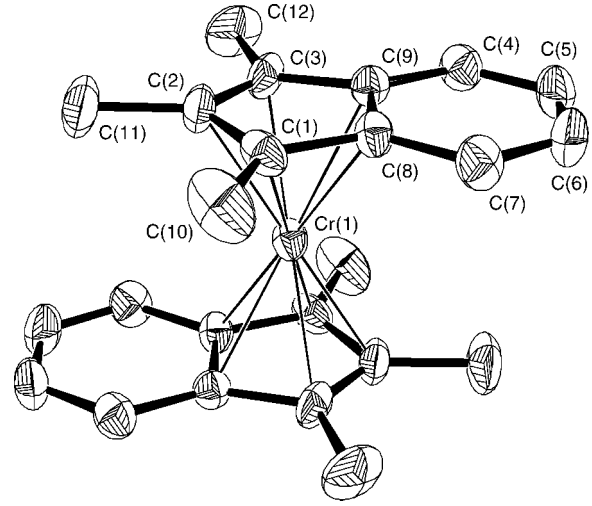

Figure 6. ORTEP drawing of the non-hydrogen atoms of $(Ind^{3Me\text{-}1,2,3})_2Cr$ at 173 K, illustrating the numbering scheme used in the text. Thermal ellipsoids are shown at the 50% level.

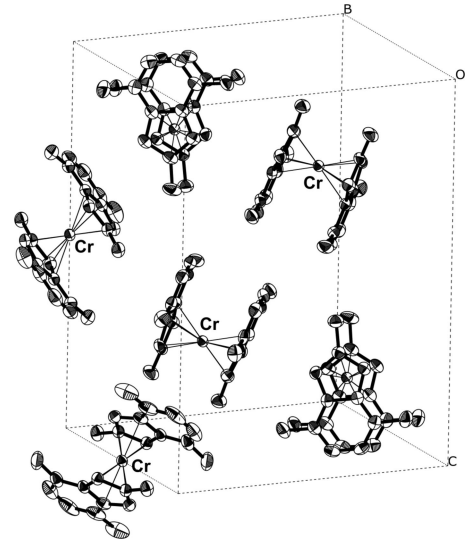

Figure 7. Unit cell of the non-hydrogen atoms of $(Ind^{3Me\text{-}2,4,7})_2Cr$ at 173 K, illustrating the cocrystallized eclipsed and staggered forms. Thermal ellipsoids are shown at the 50% level.

173 K Data. Staggered Structure (Figure 8). The Cr−C ring distances (average 2.172(4) Å) are indicative of a low-spin chromium(II) center; other low-spin species in this series display average Cr−C bond distances between 2.18 and 2.22 Å. A small degree of slippage (Δ_{M-C} = 0.076 Å) is observed

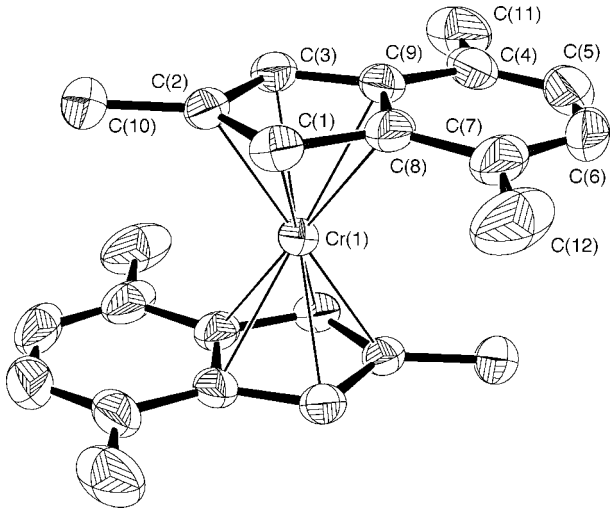

Figure 8. ORTEP drawing of the non-hydrogen atoms of staggered $(Ind^{3Me\text{-}2,4,7})_2Cr$ at 173 K, illustrating the numbering scheme used in the text. Thermal ellipsoids are shown at the 50% level.

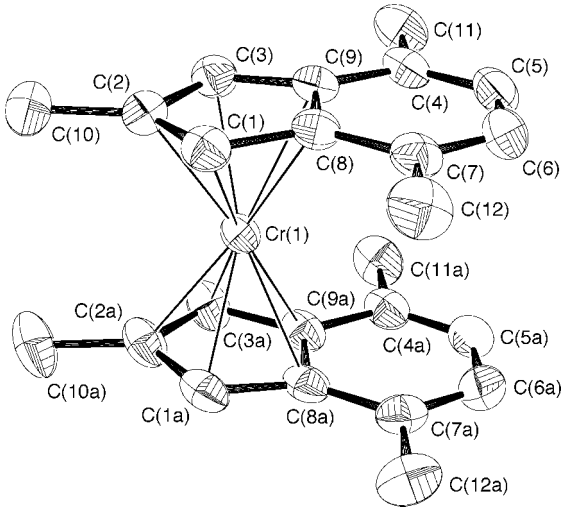

Figure 9. ORTEP drawing of the non-hydrogen atoms of eclipsed $(Ind^{3Me\text{-}2,4,7})_2Cr$ at 173 K, illustrating the numbering scheme used in the text. Thermal ellipsoids are shown at the 50% level.

Table 4. Selected Bond Distances (Å) and Angles (deg) for Staggered $(Ind^{3Me\text{-}2,4,7})_2Cr$ (173 K)

Distances			
Cr(1)−C(1)	2.1405(17)	Cr(1)−C(8)	2.2154(17)
Cr(1)−C(2)	2.1241(16)	Cr(1)−C(9)	2.2291(18)
Cr(1)−C(3)	2.1520(18)		

Angles	
inter-C_5 ring plane angle	0.0
hinge angle[a]	1.6
fold angle[a]	2.6

[a] For definitions of this angle, see ref 11.

within the complex, a result consistent with other low-spin Ind'_2Cr complexes.[11] The methyl substituent at the 2-carbon is bent 4.0° out of plane relative to the five-membered ring.

Eclipsed Structure (Figure 9). The Cr−C ring distances (average 2.168(5) Å) are among the shortest observed in the substituted Ind'_2Cr series and are consistent with a low-spin chromium(II) center. The small degree of slippage (Δ_{M-C} = 0.078 Å) observed with the ligands is similar to values found in other low-spin Ind_2Cr complexes.[11] The rings are oriented in an almost perfectly eclipsed configuration, with a twist angle of 1.9°. Relative to the C_5 ring, the methyl substituent at C(2) displays pronounced distortion, with an average out-of-plane bending angle of 6.7°.

Table 5. Selected Bond Distances (Å) and Angles (deg) for Eclipsed $(Ind^{3Me\text{-}2,4,7})_2Cr$ (173 K)

Distances			
Cr(1)−C(1)	2.1427(18)	Cr(1)−C(1a)	2.1432(18)
Cr(1)−C(2)	2.1248(17)	Cr(1)−C(2a)	2.1218(18)
Cr(1)−C(3)	2.1331(17)	Cr(1)−C(3a)	2.1419(17)
Cr(1)−C(8)	2.2234(17)	Cr(1)−C(8a)	2.2167(17)
Cr(1)−C(9)	2.2147(17)	Cr(1)−C(9a)	2.2166(16)

Angles	
inter-C_5 ring plane angle	9.7
hinge angle[a]	1.8(av)
fold angle[a]	4.3(av)
twist	1.9

[a] For definitions of this angle, see ref 11.

Table 6. Selected Bond Distances (Å) and Angles (deg) for Staggered $(Ind^{3Me\text{-}2,4,7})_2Cr$ (293 K)

Distances			
Cr(1)−C(1)	2.186(2)	Cr(1)−C(8)	2.280(3)
Cr(1)−C(2)	2.185(3)	Cr(1)−C(9)	2.294(3)
Cr(1)−C(3)	2.190(3)		

Angles	
inter-C_5 ring plane angle	0.0
hinge angle[a]	3.8
fold angle[a]	3.3

[a] For definitions of this angle, see ref 11.

Table 7. Selected Bond Distances (Å) and Angles (deg) for Eclipsed $(Ind^{3Me\text{-}2,4,7})_2Cr$ (293 K)

Distances			
Cr(1)−C(1)	2.154(3)	Cr(1)−C(1a)	2.157(3)
Cr(1)−C(2)	2.140(3)	Cr(1)−C(2a)	2.145(3)
Cr(1)−C(3)	2.144(3)	Cr(1)−C(3a)	2.155(3)
Cr(1)−C(8)	2.247(3)	Cr(1)−C(8a)	2.240(2)
Cr(1)−C(9)	2.246(3)	Cr(1)−C(9a)	2.238(2)

Angles	
inter-C_5 ring plane angle	7.6
hinge angle[a]	2.7(av)
fold angle[a]	3.2(av)
twist	2.0

[a] For definitions of this angle, see ref 11.

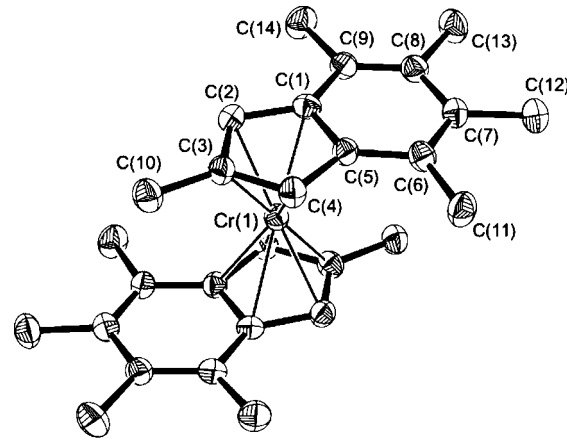

Figure 10. ORTEP drawing of the non-hydrogen atoms of eclipsed $(2,4,5,6,7\text{-}Me_5C_9H_2)_2Cr$ at 173 K, illustrating the numbering scheme used in the text. Thermal ellipsoids are shown at the 50% level.

293 K Data. Staggered Structure. The Cr−C ring distance (average 2.227(6) Å) has lengthened significantly upon warming to 293 K; it is 0.0546 Å longer than that observed for the same

Table 8. Selected Bond Distances (Å) and Angles (deg) for (2,4,5,6,7-Me$_5$C$_9$H$_2$)$_2$Cr

Distances			
Cr(1)−C(1)	2.221(4)	Cr(1)−C(4)	2.133(5)
Cr(1)−C(2)	2.146(4)	Cr(1)−C(5)	2.218(4)
Cr(1)−C(3)	2.124(4)		

Angles	
inter-C$_5$ ring plane angle	4.3
hinge angle[a]	2.0
fold angle[a]	2.9

[a] For definitions of this angle, see ref 11.

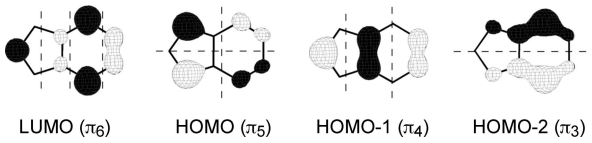

Figure 11. Frontier π orbitals of the indenyl anion. The π_n notation is the same as that used by previous authors.[36]

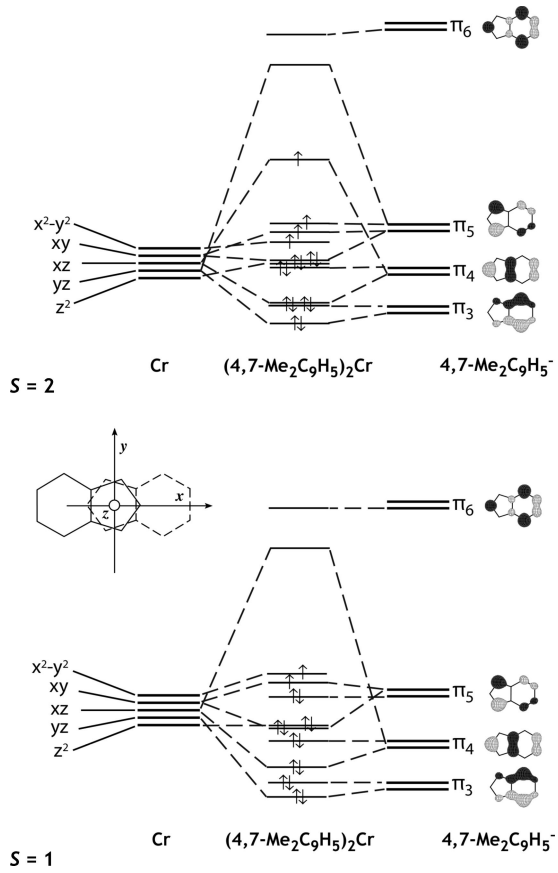

Figure 12. MO diagrams for the hypothetical high-spin (top) and low-spin (bottom) staggered (Ind$^{2Me\text{-}4,7}$)$_2$Cr complex.

conformer at 173 K. The ring slippage (Δ_{M-C} = 0.099 Å) is now more pronounced (by 27%) than at the lower temperature. Distortion of the methyl group at the 2-carbon relative to the C$_5$ ring is similar to that observed at 173 K, with an average out-of-plane bending angle of 3.9°.

Eclipsed Structure. The Cr−C ring distance (average 2.187(9) Å) lengthens only slightly (0.0186 Å) when the species is warmed to 293 K from 173 K, about one-third of the elongation observed in the staggered structure. The ring slippage (Δ_{M-C} = 0.091 Å) is slightly more pronounced than what was observed in the low-temperature structure, but the twist angle (2.0°) remains essentially unchanged. The canting of the rings has decreased from 9.7° to 7.8°. The methyl substituent at the 2-carbon is still substantially displaced from the C$_5$ ring plane (5.9° average), but slightly less than at 173 K.

(2,4,5,6,7-Me$_5$C$_9$H$_2$)$_2$Cr. Crystals of (2,4,5,6,7-Me$_5$C$_9$H$_2$)$_2$Cr were obtained as blocks from a slowly evaporated hexanes solution. Only half of each molecule is unique, as the metal lies on a crystallographically imposed 2-fold axis. An ORTEP drawing is provided in Figure 10, displaying the numbering scheme used in the text; selected bond lengths and angles are shown in Table 8. Although they are not required to be so, the indenyl ligands are almost perfectly staggered, with a twist angle of 179.2°. It might be possible that CH/π interactions assist in the alignment of the ligands,[31] but the closest intramolecular C$_{Me}$···C$_{sp^2}$ distance (C(10)−C(7′)) is only 3.70 Å. This matches the sum of the van der Waals radii for CH$_3$ (2.0 Å) and C$_{sp^2}$ (1.7 Å). All methyl group contacts lie outside the sum of van der Waals radii (4.0 Å).There are no C$_{sp^2}$···H contacts closer than the sum of the appropriate radii (3.9 Å).

The average Cr−C ring distance of 2.17(1) Å is indicative of a low-spin chromium(II) center; it closely resembles those found in low-spin bis(indenyl) complexes of chromium(II), e.g., (Ind^{7Me})$_2$Cr (2.18(2) Å),[11] (Ind^{2tBu})$_2$Cr (2.22(2) Å), and (Ind^{2Si})$_2$Cr (2.20(2) Å).[9] The slip parameter (Δ_{M-C} = 0.080 Å) is also typical for low-spin Ind′$_2$Cr complexes.[11]

Discussion

Molecular symmetry and electron donation from the ligands interact in complex ways in bis(indenyl)chromium(II) complexes. Largely unpredictable crystal-packing forces have a prominent effect on the former, and some instances of spin-crossover behavior are observed only in the solid state, where intermolecular cooperative effects are operative. In this regard, it is notable that staggered and eclipsed conformations are the only arrangements found in the solid state with the methylated compounds; the gauche arrangements observed in [1,3-(*t*-Bu or SiMe$_3$)$_2$C$_9$H$_5$]$_2$Cr appear to require the presence of groups more sterically demanding than methyl or even isopropyl.[9]

The eight known bis(indenyl)chromium(II) compounds with methylated ligands comprise a set in which several trends involving ligand conformation, substitution, and magnetic properties are evident. Owing to the compact size of methyl groups, intramolecular steric interactions are not significant here. Instead, the two most clearly defined patterns are the following.

(1) *Symmetry is an important, but not completely determinant, influence on the spin state*. There is now strong empirical and computational evidence that a staggered ligand conformation (specifically, one with C_i symmetry) supports a high-spin state in bis(indenyl)chromium(II) complexes, that an eclipsed conformation is less supportive (and associated with spin-crossover molecules), and that a twisted (gauche) conformation is associated with low-spin molecules.[9,14] That the symmetry restrictions are not absolute is indicated by (Ind^{7Me})$_2$Cr, which is staggered in the solid state but at all measured temperatures is low spin.

(2) *Increasing methylation supports a lower spin state*. Apart from symmetry effects, it is apparent that more complete methylation is associated with lower spin state molecules. Between the extremes of (Ind^{7Me})$_2$Cr and (Ind$^{Me\text{-}2}$)$_2$Cr are molecules that undergo thermally induced spin crossovers. This phenomenon is reminiscent of that of manganocene, Cp$_2$Mn, and its ring-substituted derivatives. The parent compound is high spin (S = $^5/_2$; 5.50 μ_B) at 373 K, but converts to a low-spin

(31) Nishio, M.; Hirota, M.; Umezawa, Y. *The CH/π Interaction: Evidence, Nature, and Consequences*,; Wiley-VCH: New York, 1998.

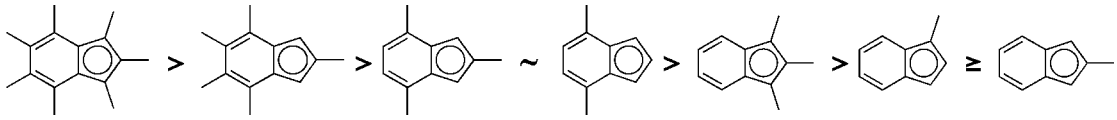

Figure 13. Association of methylated indenyl ligands with low-spin ground states in bis(indenyl)chromium(II) complexes.

species ($S = {}^1/_2$; 1.99 μ_B) at lower temperatures (193 K).[32] Alkylation of the cyclopentadienyl ring increases the d-orbital splitting and preference for spin pairing, so that $(C_5Me_5)_2Mn$, for example, is low spin (2.18 μ_B) over a large temperature range.[13]

In the case of the molecules discussed here, the exact type of behavior observed (i.e., whether the spin transitions are complete or not) is a function not only of the number of substituents but also of their *location* on the indenyl ligand. The way in which symmetry and the degree/location of methylation affects the magnetic properties can be summarized as follows.

$(Ind^{Me\text{-}2})_2Cr$. This is the most straightforward case, as the molecule is minimally substituted, adopts a staggered conformation in the solid state, and is high spin both in solution and in the solid state at all temperatures.[14]

$(Ind^{Me\text{-}1})_2Cr$. Although the molecule exhibits spin-crossover behavior in the solid state, this is certainly the result of its eclipsed configuration, which is dictated by crystal-packing forces. In solution, it is high spin and likely adopts a staggered conformation.[14]

$(Ind^{3Me\text{-}1,2,3})_2Cr$. This molecule demonstrates the increasing effect of ligand methylation, as it displays spin-crossover behavior in the solid state, despite its staggered configuration. Nevertheless, it is high spin in solution, indicating that, even with the front ring completely methylated, cooperative effects in the solid state are necessary to overcome the symmetry-imposed preference for a high-spin state.

$(Ind^{3Me\text{-}2,4,7})_2Cr$ and $(Ind^{2Me\text{-}4,7})_2Cr$. Conceptually, $(Ind^{3Me\text{-}2,4,7})_2Cr$ can be derived from $(Ind^{3Me\text{-}1,2,3})_2Cr$ by moving two methyl groups to the benzo ring. The fact that both eclipsed and staggered conformations are found in the solid state is a consequence of crystal packing but also indicates that they are essentially equienergetic. In solution, a magnetic moment not characteristic of either high spin or low spin is observed, suggesting that comparable populations of eclipsed and staggered conformations are present in spin equilibrium. $(Ind^{2Me\text{-}4,7})_2Cr$ has a similar magnetic moment in solution, indicating that the single methyl group on the five-membered ring plays a minor role in determining the magnetic behavior. The fact that the latter is eclipsed in the solid state produces its spin-crossover behavior, which is similar to that of the eclipsed $(Ind^{Me\text{-}1})_2Cr$.[14]

As the number of methyl groups is the same in $(Ind^{3Me\text{-}2,4,7})_2$-Cr and $(Ind^{3Me\text{-}1,2,3})_2Cr$, the former's lower magnetic moment in solution is clearly related to the location of the methyl groups on the ligands. The data suggest that substitution on the benzo ring has at least as strong an influence on spin state as when substitution occurs on the five-membered ring. Solid-state data are also consistent with this; to the extent that increasing methylation supports a low-spin state, it can be noted that the average Cr−C distance in the staggered conformation of $(Ind^{3Me\text{-}2,4,7})_2Cr$ at 173 K (2.172(4) Å) is 3% shorter than that in the staggered $(Ind^{3Me\text{-}1,2,3})_2Cr$ (2.239(11) Å) at the same temperature. It should be pointed out that similar positional effects have not been observed in the UV/vis or cyclic voltammetry (CV) data of methyl-substituted bis(indenyl)iron(II) complexes;[33] the UV/vis data are relatively insensitive to the substitution pattern (a consequence of an essentially constant HOMO/LUMO gap), and the CV data reflect the energy of the HOMO only, for which substitution on the benzo ring has less of an effect than methylation on the five-membered ring.

Consideration of the HOMO-*n* orbitals of the indenyl anion (Figure 11) makes it apparent that substitution on the 4,7-position should most strongly affect the energy of the LUMO (π_6), HOMO (π_5), and HOMO-2 (π_3) orbitals. Although the last orbital is sometimes considered not to be substantially involved in bonding in transition-metal bis(indenyl) complexes,[34] calculations on the $[Ind^{2Me\text{-}4,7}]^-$ anion (TPSSh/6-31+G(d)) indicate that the energy of the π_3 orbital is raised by 0.30 eV relative to the unsubstituted anion; in contrast, the energy of π_4 is lowered, but by only 0.02 eV.[35]

To determine how these changes affect the molecular orbitals of a complex, calculations were performed at the TPSSh/6-31+G(d) level on high- and low-spin Ind_2Cr and $(Ind^{2Me\text{-}4,7})_2Cr$ (see the Supporting Information for additional details). The Ind_2Cr diagrams are similar to that calculated at the B3PW91/LANL2DZ level for the unsubstituted complex.[9] There are many closely spaced energy levels in the diagrams for $(Ind^{2Me\text{-}4,7})_2Cr$ (Figure 12), but no truly degenerate molecular orbitals ($\Delta E \geq 0.04$ eV). For the staggered $(Ind^{2Me\text{-}4,7})_2Cr$ complex that is calculated in the high-spin state, the π_3-associated orbitals are raised to within 0.05 eV of those associated with π_4. This in turn affects the π_4/d_{xz} orbitals, raising the energy of the bonding combination and conversely lowering the energy of the antibonding combination, which is the HOMO. If the molecule is placed in the low-spin state, the π_3 orbitals drop in energy, with a gap of 0.34 eV below the π_4/d_{xz} combination. The reduced electron repulsion has the effect of lowering the energy of the entire molecule by 2.4 kJ mol^{-1}, a small amount consistent with spin-crossover effects.[2]

$(2,4,5,6,7\text{-}Me_5C_9H_2)_2Cr$ and $(Ind^{7Me})_2Cr$. The high degree of methylation in both these molecules is responsible for their completely ($(Ind^{7Me})_2Cr$) or mostly ($(2,4,5,6,7\text{-}Me_5C_9H_2)_2Cr$) low-spin states, despite their staggered conformations. The fact that the removal of two of the methyl groups from the five-membered ring allows $(2,4,5,6,7\text{-}Me_5C_9H_2)_2Cr$ to undergo an incomplete crossover underscores the persistence of the symmetry effects in the complexes, even with substantial methylation. Rotation of $(2,4,5,6,7\text{-}Me_5C_9H_2)_2Cr$ to a partially eclipsed conformation in solution would reinforce the low-spin state.

(32) Switzer, M. E.; Wang, R.; Rettig, M. F.; Maki, A. H. *J. Am. Chem. Soc.* **1974**, *96*, 7669–7674.

(33) Curnow, O. J.; Fern, G. M. *J. Organomet. Chem.* **2005**, *690*, 3018–3026.

(34) O'Hare, D.; Green, J. C.; Marder, T.; Collins, S.; Stringer, G.; Kakkar, A. K.; Kaltsoyannis, N.; Kuhn, A.; Lewis, R.; Mehnert, C.; Scott, P.; Kurmooo, M.; Pugh, S. *Organometallics* **1992**, *11*, 48–55.

(35) This conclusion is relatively insensitive to the level of theory employed. With the B3LYP functional and the larger aug-cc-pVTZ basis set, for example, the energy of the π_3 orbital of the $[Ind^{2Me\text{-}4,7}]$ anion is raised by 0.33 eV relative to the unsubstituted anion; the energy of π_4 is lowered by 0.02 eV.

(36) Crossley, N. S.; Green, J. C.; Nagy, A.; Stringer, G. *J. Chem. Soc., Dalton Trans.* **1989**, 2139–2147.

Taking all the solution and solid-state magnetic measurements into account, the approximate association of methylated indenyl ligands with low-spin ground states can be summarized as in Figure 13.

Conclusions

We have shown that rational design of substituted indenyl ligands can lead to bis(indenyl)chromium(II) complexes that exhibit high-spin, low-spin, and spin-crossover behavior. The number and location of substituents on the indenyl ligands, coupled with molecular symmetry restrictions, generate large windows for manipulating the magnetic ground state. In addition to the preference for high-spin states imposed by centrosymmetric molecules and the countervailing tendency for low-spin states provided by increasing methylation of the ring, the specific location of methyl groups on the ligands has a substantial effect on the magnetic properties of the complexes.

Benzo-ring substitution has a greater stabilizing effect on the low-spin state than comparable substitution on the five-membered ring. Given the latter's proximity to the metal, this is not an immediately intuitive result but can be understood as stemming from the peculiar electronic features of the π-orbitals of the indenyl anion. The tunability of the magnetic properties of bis(indenyl)metal complexes with site-specific ligand substitution has implications in the construction of charge transfer salts.[15] It more broadly hints at the significant electronic (as distinct from steric) modifications that could be exploited with indenyl ligands that are used in polymerization catalysts.[37]

Acknowledgment. We thank the donors of the Petroleum Research Fund, administered by the American Chemical Society, for support of this research and the NSF for partial funding of the SQUID magnetometer. E.D.B. was supported with a GAANN Fellowship from the Department of Education. Guangbin Wang is thanked for help with the magnetic measurements.

Supporting Information Available: CIF files giving X-ray crystallographic data for $(2,4,5,6,7\text{-}Me_5C_9H_2)_2Cr$, $(Ind^{3Me\text{-}1,2,3})_2Cr$, $(Ind^{2Me\text{-}4,7})_2Cr$, $(Ind^{3Me\text{-}2,4,7})_2Cr$ (173 and 293 K) and figures and text giving SQUID data for $(2,4,5,6,7\text{-}Me_5C_9H_2)_2Cr$, additional computational details, and the complete ref 23. This material is available free of charge via the Internet at http://pubs.acs.org.

OM800473Z

(37) Calhorda, M. J.; Felix, V.; Veiros, L. F. *Coord. Chem. Rev.* **2002**, *230*, 49–64.